# BUNDLE BLOCK ADJUSTMENT OF CBERS 2B HRC IMAGES USING CONTROL LINES

J. Marcato Junior [a], A. M. G. Tommaselli [a], N. G. Medeiros [b], R. A. Oliveira [a]

[a] Dept. of Cartography, Unesp - Univ Estadual Paulista, 19060-900 Pres. Prudente, SP, Brazil - jrmarcato@gmail.com, tomaseli@fct.unesp.br, raquel88@gmail.com
[b] Dept. Of Civil Engineering, Universidade Federal de Viçosa - UFV, 36570-000 Viçosa, MG, Brazil – nilcilene.medeiros@ufv.br

**KEY WORDS:** Photogrammetry, Orbital images, Straight lines, Image Orientation, Pushbroom, CBERS images

**ABSTRACT:**
China-Brazil Earth Resources Satellite (CBERS) images present strategic importance for Brazil, providing support in several applications such as deforestation management and fire control, mainly in Amazon region. CBERS 2B carries three imagery sensors: High Resolution Camera (HRC), CCD Camera and Wide Field Imager (WFI), which provide images with GSD of 2.5 meters (m), 20 m and 260 m, respectively. One problem with these images is the accuracy of their georreferencing, being necessary to correct them with ground control information. Although points are generally used as control elements in spatio-triangulation, some advantages motivate the use of linear features in Photogrammetry, including the plenty of this feature in man-made environments and the improvement of the robustness and geometric strength in bundle block adjustment. The aim of this work is to experimentally assess a block adjustment method based on linear features with CBERS 2B HRC images. The model being used states the coplanarity condition between the projection ray in the image and the projection plane in the object space. This model was implemented in the TMS (Triangulation with multi sensors) software that uses multifeatures control (points and lines). Experiments using a block composed by four CBERS 2B HRC images from two adjacent orbits were carried out and the results showed that the model based on straight lines works successfully in spatio-triangulation with CBERS 2B HRC images providing better results when compared to those obtained by triangulation with collinearity model, based on points.

## 1. INTRODUCTION

Bundle block adjustment with satellite images, also known as spatio-triangulation, was firstly developed and tested in the eighties with SPOT across-track stereo images (Toutin and Rochon, 1986). Ever since several works have approached the application of this process for images collected by different satellites such as Landsat, Kompsat, QuickBird and ALOS (Toutin, 2003; Poli, 2005; Kim and Dowman, 2006; Kocaman and Gruen, 2008).

China-Brazil Earth Resources Satellite (CBERS) images present strategic importance for Brazil, providing support in several applications including deforestation management and fire control, mainly in Amazon region. Another motivation is that CBERS images of South American and African territory are freely distributed. The third generation satellite CBERS 2B, which is the current satellite in orbit, carries three imagery sensors: High Resolution Camera (HRC), CCD Camera and Wide Field Imager (WFI). HRC images have a GSD of 2.5 meters (m), but this camera presents a large temporal resolution, 130 days (INPE, 2010). This camera does not provide stereoscopic coverage, however, images acquired from adjacent orbits (east – west) present an overlap with a base-to-height (B/H) ratio of around 0.13, providing a weak intersection geometry.

Toutin (2003) accomplished experiments applying the bundle block adjustment method for nadir viewing Landsat 7 ETM+ images. In this research 15 images were used, with a B/H ratio of around 0.12 to 0.14, for images acquired from adjacent orbits. Even in this case, where the B/H ratio is less than 0.60, some advantages motivate the application of bundle block adjustment instead of performing the single image orientation, including the reduction of Ground Control Points (GCPs) and the achievement of a better relative accuracy (Toutin, 2003).

One problem with CBERS 2B HRC images is the accuracy of their georreferencing, mainly caused by attitude angles errors (Yu et al. 2008). Yu et al. (2008) presented a calibration model in order to eliminate constant angular errors with sparse control. Even applying this method, errors around 20 GSDs in the check points were achieved, which can be considered a large value.

Considering that, it is necessary to correct these images with dense ground control elements, such as points or lines. Although points are generally used as control elements in spatio-triangulation, some advantages motivate the use of linear features in Photogrammetry (Tommaselli and Tozzi, 1996; Habib and Morgan, 2003):

- Plenty of this feature in man-made environments;
- Improvement of the robustness and geometric strength in bundle block adjustment;
- Extraction of image lines with sub-pixel accuracy;
- The correspondence between points from image and object lines is not necessary.

Besides, Habib et al. (2001) showed that the use of straight lines elements in the triangulation of images acquired by linear array scanners provides a better recovery of the EOPs (Exterior Orientation Parameters) when compared to those methods that use distinct points.

The aim of this work is to experimentally assess a block adjustment method based on linear features with CBERS 2B HRC images and to present the current achievements of the TMS (Triangulation with multi sensors) project.

## 2. BACKGROUND

### 2.1 Mathematical model using straight lines

The Line Coplanarity Model (LCM) using straight lines is based on the coplanarity between the projection ray containing an image point ($v_i$) and the projection plane in the object space, defined by a ground line and the instantaneous perspective centre. As a result, the vector normal to the projection plane in the object space must be orthogonal to the projection ray (Fig. 1) in an auxiliary system. This auxiliary system is obtained by applying the inverse rotation matrix to the image (photogrammetric) reference system, which makes it parallel to the object space reference system.

In Figure 1, the straight line in the object space is defined by $P_1$ and $P_2$ and $p_i$ is a point in the corresponding image line for a specific image row j. It is important to notice that the correspondence between points from the image and object space is not necessary. The concept of this model is the same as presented by Mulawa and Mikhail (1988) and Habib et al. (2002), with small differences in notation.

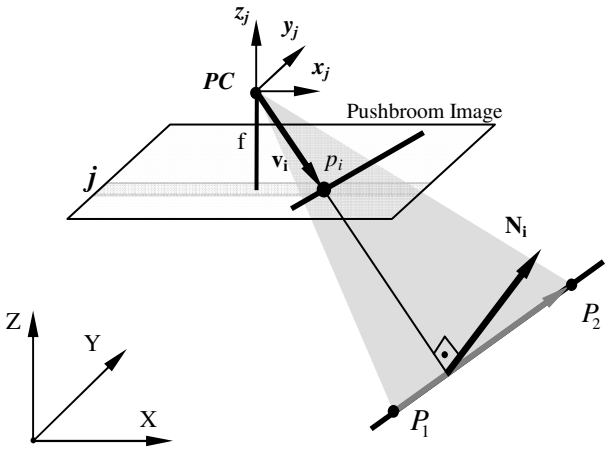


Figure 1. The projection ray and the vector normal to the projection plane in the object space.

The orthogonality condition between the projection ray ($v_i$) in the auxiliary reference system and the vector normal to the projection plane in the object space ($N_i$) can be expressed by Equation 1. Considering the y axis oriented in the orbit direction, this coordinate is null for an instant t, corresponding to an image row j.

$$\mathbf{N}_i \mathbf{R}_\mathbf{j}^\mathbf{T} \begin{bmatrix} x_i \\ 0 \\ -f \end{bmatrix} = 0 \tag{1}$$

where: $N_i$ is the vector normal to the projection plane in the object space defined by the cross product of the direction vector $(\boldsymbol{P_2 - P_1})$ of the straight line and the vector difference between the instantaneous Perspective Centre and point $P_1$ in the object straight line $(\boldsymbol{P_C - P_1})$ (see Fig. 1); $[x_i, 0, -f]^T$ is the position vector of point $p_i$ in the image space (projection ray); $f$ is the camera focal length and; $Rj^T$ is the inverse rotation matrix for the photogrammetric reference system corresponding to an image row j. The rotation matrix is defined by:

$$R_j = \begin{bmatrix} \cos\kappa_s & \cos\omega\cdot\sin\kappa_s & \sin\omega\cdot\sin\kappa_s \\ -\sin\kappa_s & \cos\omega\cdot\cos\kappa_s & \sin\omega\cdot\cos\kappa_s \\ 0 & -\sin\omega & \cos\omega \end{bmatrix} \tag{2}$$

The rotation matrix $R_j$ equation makes the object and image reference systems parallel. In this matrix, the rotation angle $\varphi$ is considered null due to its correlation with $X_0$, and $\omega$ rotation is considered a constant value. Finally, the Line Coplanarity Model is given by:

$$\begin{aligned} &[\Delta Y(Z_1 - Z_S) - \Delta Z(Y_1 - Y_S)](\cos\kappa x_i) + \\ &+[\Delta Z(X_1 - X_S) - \Delta X(Z_1 - Z_S)](\cos\omega\sin\kappa x_i - \sin\omega f) + \\ &+[\Delta X(Y_1 - Y_S) - \Delta Y(X_1 - X_S)](\sin\omega\sin\kappa x_i - \cos\omega f) = 0 \end{aligned} \tag{3}$$

In Equation 3, the EOPs are described by second-order polynomials (Orun and Natarajan, 1994):

$$\begin{aligned} X_S &= X_0 + a_1 t + b_1 t^2 \\ Y_S &= Y_0 + a_2 t + b_2 t^2 \\ Z_S &= Z_0 + a_3 t + b_3 t^2 \\ \kappa &= \kappa_0 + a_4 t + b_4 t^2 \end{aligned} \tag{4}$$

where:

- $X_0$, $Y_0$, $Z_0$ are the perspective centre coordinates for the first image row;
- $\kappa_0$ is the rotation angle around Z-axis for the first image row;
- $a_i$ and $b_i$ are polynomial coefficients;
- $t$ is a time-dependent parameter;
- $X_s$, $Y_s$, $Z_s$, $\kappa$ are the values interpolated with Equation 4, which corresponds to the EOPs for each image row ($j$).

A detailed description about this model is presented in Tommaselli and Medeiros (2010).

### 2.2 Collinearity model

The Collinearity Model for pushbroom sensor (CMP) was developed based on the collinearity condition between a point in the object space, its homologous in the image space and the instantaneous perspective centre (PC) corresponding to the image row that contains this point. Equations 5 are the Collinearity Model for the pushbroom geometry (Light et al., 1980).

$$x_i = -f\frac{r_{11}(X_i - X_S) + r_{12}(Y_i - Y_S) + r_{13}(Z_i - Z_S)}{r_{31}(X_i - X_S) + r_{32}(Y_i - Y_S) + r_{33}(Z_i - Z_S)} \quad (5)$$

$$0 = y_i = -f\frac{r_{21}(X_i - X_S) + r_{22}(Y_i - Y_S) + r_{23}(Z_i - Z_S)}{r_{31}(X_i - X_S) + r_{32}(Y_i - Y_S) + r_{33}(Z_i - Z_S)}$$

where: $x_i$ is the instantaneous image coordinate for a point in row i; $X_i$, $Y_i$, $Z_i$ are the 3D coordinates of the corresponding point in the object space and; $X_s$, $Y_s$, $Z_s$ and $r_{ij}$ were previously defined in section 2.1.

## 3. METHODOLOGY

In order to assess the block triangulation method based on linear features, outlined in section 2.1, experiments with a block composed by four level 1(with only radiometric correction) CBERS 2B HRC images were performed. These images are from adjacent orbits (159 and 158). The images 159-E_125-1 and 159-E_125-2 were collected in the same day, however 158-A_125-1 and 158-A_125-A images were acquired in different dates.

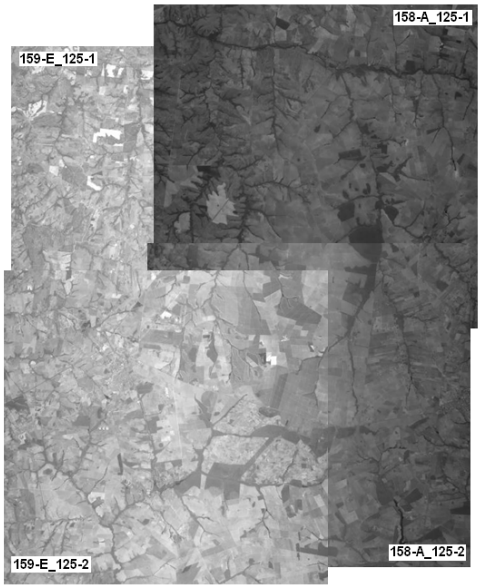


Figure 2. Block composed by CBERS-2B HRC images.

The focal length value of HRC was fixed in the bundle block adjustment. Besides the focal length value, some technical features about HRC are presented in Table 1.

| | |
|---|---|
| Focal length (mm) | 3398 |
| Image level | 1 (radiometric correction) |
| Image size (pixels) | 12246x12246 |
| GSD (m) | 2.5 |
| Orbital altitude (km) | 778 |

Table 1. Technical features of CBERS-2B HRC (INPE, 2010; Machado e Silva, 2007).

The control points and lines were surveyed with a dual-frequency GPS, Hipper GGD. The GPS data were processed using the PPP (Precise Point Positioning) online service available at IBGE (Instituto Brasileiro de Geografia e Estatística) web site. Object space linear features were defined by endpoints directly measured on road centre lines with GPS in cinematic mode.

After the processing of GPS data, collected in cinematic mode, the resulting coordinates were filtered in order to remove points with a high standard deviation and to establish representative coordinates for each road segment. In this last step it was applied a 3D collinearity condition among the road points, in order to ensure that the points are truly part of a straight line. Figure 3 depict this condition. To verify whether or not the point $P_3$ belongs to the straight line, defined by points $P_1$ and $P_2$, the orthogonal length (L) of point ($P_3$) to the straight line and the vertical (θ) and horizontal (α) angles were calculated. Thus, establishing proper thresholds it is possible to check if the point actually belongs to the straight line. After this analysis, the coordinates of the road centre were calculated applying an offset, which was estimated through the car trajectory along both directions of the road.

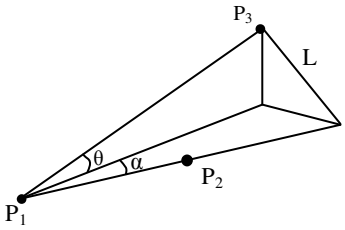


Figure 3. Collinearity condition applied to road control points.

Experiments using both models, Collinearity (CMP) and Coplanarity (LCM), for block adjustment were carried out. The models were implemented in the in-house developed TMS software that uses multifeatures control (points and lines). It is important to mention that this software uses the Combined Least Square Method in the adjustment process (Mikhail and Ackerman, 1976).

## 4. EXPERIMENTS AND RESULTS ANALYSIS

Table 2 characterizes the experiments carried out in this section. Figures 4 and 5 show, respectively, the control points and lines distribution along the block. In the experiments the results obtained with combination of GCPs (Ground Control Points) and GCLs (Ground Control Lines) with TPs (Tie Points) and ZoCPs (Z only Control Points) were assessed.

| Experiments | Ground Control Points (GCPs) | Tie Points (TPs) | Z only Control Points (ZoCPs) | Ground Control Lines (GCLs) |
|---|---|---|---|---|
| A | 78 | 0 | 0 | 0 |
| B | 78 | 44 | 0 | 0 |
| C | 78 | 0 | 44 | 0 |
| D | 0 | 0 | 0 | 113 |
| E | 0 | 44 | 0 | 113 |
| F | 0 | 0 | 44 | 113 |

Table 2. Experiments configuration.

The Z only control points (see Figure 6), also known as Elevation Tie Points – ETPs (Toutin, 2003), are points that have their elevation previously known. In experiments C and F

the elevation of these points were obtained from the SRTM (Shuttle Radar Topography Mission).

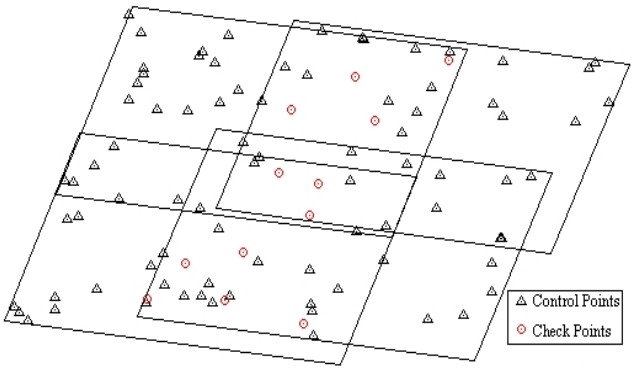


Figure 4. Control and Check points configuration.

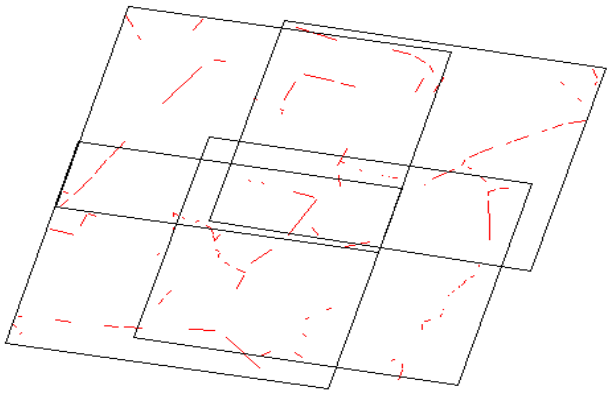

Figure 5. Control lines configuration.

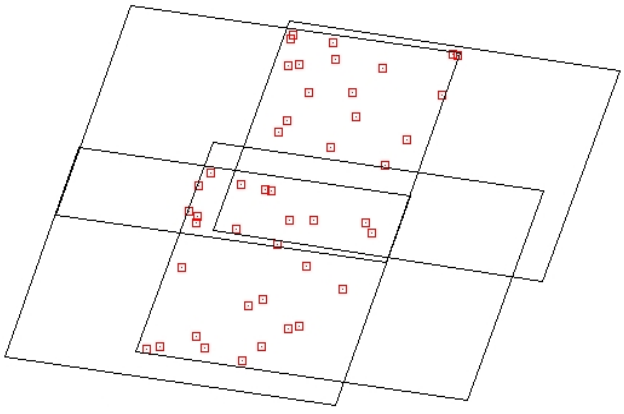

Figure 6. Tie points and Z only control points configuration.

Table 3 and Figure 7 present the Root Mean Square (RMS) in the check points coordinates (12 points showed in Figure 4). These coordinates were calculated after the bundle block adjustment using the photogrammetric intersection procedure.

| Exp. | X(m) | Y(m) | X(GSD) | Y(GSD) |
|---|---|---|---|---|
| A | 4.5 | 8.6 | 1.8 | 3.4 |
| B | 5.0 | 7.5 | 2.0 | 3.0 |
| C | 4.7 | 7.6 | 1.9 | 3.0 |
| D | 4.8 | 6.1 | 2.0 | 2.4 |
| E | 5.0 | 4.5 | 2.0 | 1.8 |
| F | 5.3 | 6.0 | 2.1 | 2.4 |

Table 3. RMS in the checkpoints coordinates (Intersection).

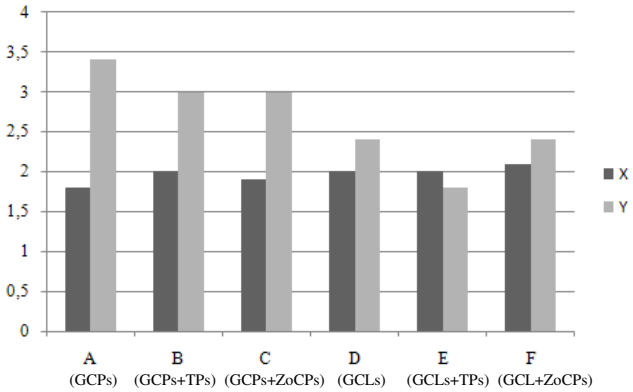


Figure 7. RMS(GSD) in the check points coordinates (Intersection).

The analysis of Table 3 and Figure 7 shows the feasibility of applying the bundle block adjustment instead of the single image orientation. This was verified through the use of TPs and ZoCPs (ETPs) in experiments B and C providing a better relative accuracy when compared with experiment A where no TPs and ZoCPs were used.

Also, it was verified in the case studied that the use of ZoCPs instead of TPs, even in this case where the B/H ratio is around 0.13, did not improve significantly the estimation of object points coordinates of check points. It was verified just a small reduction in the RMS of the X component with the introduction of ZoCP (experiment C), instead of TPs (experiment B).

From the analysis of the results obtained in experiments A and D, it was verified that the LCM model provided better results in the estimation of the Y coordinate through the intersection procedure when compared to the CMP model. The RMS in the Y coordinate was around 6.1 m (2.4 GSDs) in the LCM model whereas for the CMP this value was around 8.6 m (3.4 GSDs). Although in the bundle block adjustment more lines than points had been used, in practical terms it seems natural that the time wasted for surveying a control point should allow the surveying of several control lines.

Table 4 presents the RMS in the check points coordinates for each image and Figure 8 shows the resultant RMS of the two coordinate components (X and Y). In this case, these coordinates were computed by back-projecting image coordinates using the inverse form of the collinearity equations considering a known elevation value. This experiment was done in order to assess the results from a normal user point of view. Usually, those images are to be corrected with GCPs and then orthorectified with SRTM. The results presented in Table 4 and Figure 8 represent the final accuracy that would be achieved with such a procedure.

| | *Image 1* *RMS (GSD)* | | *Image 2* *RMS (GSD)* | | *Image 3* *RMS (GSD)* | | *Image 4* *RMS (GSD)* | |
|---|---|---|---|---|---|---|---|---|
| Exp. | X | Y | X | Y | X | Y | X | Y |
| A | 1.7 | 2.6 | 2.7 | 3.1 | 1.7 | 5.0 | 2.2 | 6.8 |
| B | 1.7 | 2.8 | 2.8 | 2.8 | 1.6 | 4.5 | 2.6 | 3.9 |
| C | 1.7 | 2.8 | 2.7 | 2.8 | 1.7 | 4.5 | 2.1 | 4.0 |
| D | 2.2 | 2.9 | 2.6 | 2.9 | 2.6 | 3.7 | 4.2 | 1.7 |
| E | 1.8 | 4.0 | 2.8 | 2.0 | 1.8 | 3.7 | 4.1 | 1.7 |
| F | 1.4 | 2.8 | 2.5 | 2.4 | 2.6 | 3.6 | 4.8 | 2.3 |

Table 4. RMS in the checkpoints coordinates (Single-Ray Backprojection with a known elevation).

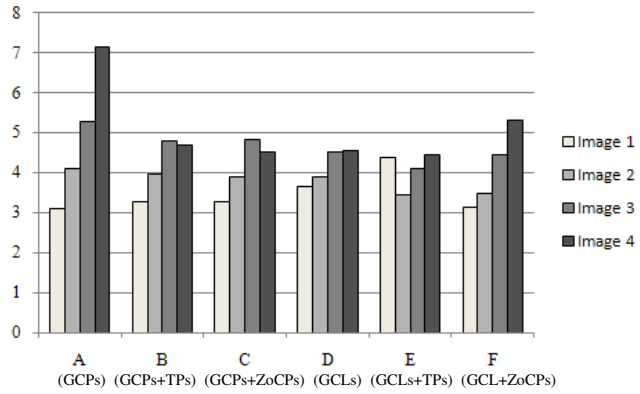


Figure 8. Resultant RMS(GSD) of XY coordinates of checkpoints for each image (Single-Ray Backprojection).

Figure 8 and Table 4 show similar results of using photogrammetric intersection:

1. Using Control lines provided better results, when compared to GCPs, mainly in Y coordinates;
2. Introducing TPs or ZoCPs improved the results in the experiments with GCPs, however;
3. the same does not apply for the experiments with control lines.

It is important to emphasize that potential causes of errors in the bundle block adjustment are related to the image points and lines distribution and measurement.

Figure 9 illustrates the histogram as well as the contrast of a point in a CBERS 2B HRC image. Observing the histogram it can be noticed that CBERS 2B HRC images present small dynamic ranges (around 40 gray values) which difficult the measurement of the image points and lines causing an error of around 1-3 pixels in this measurement process.

Besides, Carvalho et al. (2009) showed that the EIFOV (Effective Instantaneous Field of View) in along- and across-track directions for HRC images were around 4.1m and 4.6m, respectively, although the nominal GSD of CBERS 2B HRC is 2.5m.

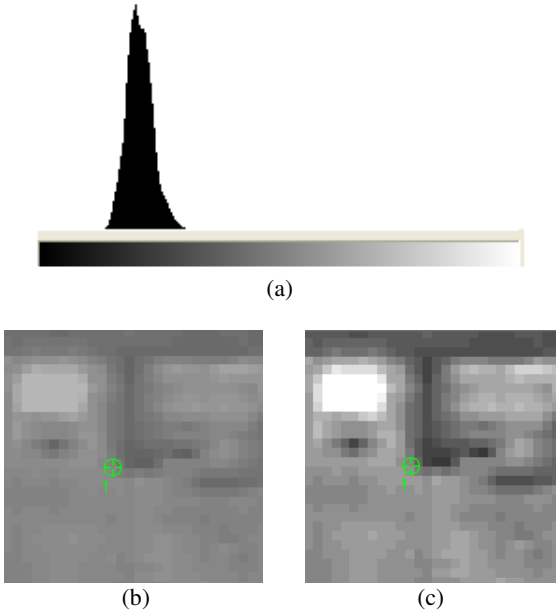

(a) (b) (c)

Figure 9. CBERS 2B HRC image. (a) Image Histogram; (b) Point definition in the original image (c) and in the contrasted image.

## 5. CONCLUSIONS

This paper presented a mathematical model based on straight lines adapted for spatio-triangulation. Experiments using both models, Collinearity (CMP) and Coplanarity (LCM), for a block composed by four CBERS 2B HRC images from two adjacent orbits were carried out. The models were implemented in the TMS software that uses multifeatures control (points and lines).

The results showed that the Line Coplanarity Model (LCM) works successfully in spatio-triangulation with CBERS 2B HRC images. Besides, it was verified the feasibility of applying the bundle block adjustment instead of the single image orientation.

Experiments combining points and lines, aiming to improve the bundle block adjustment results, will be accomplished in future research. Besides, techniques to improve and automate the measurement of image points and lines will be developed. Also, the effects of introducing orbital data in the bundle adjustment will be assessed. It is important to mention that the CBERS 2B HRC is an experimental camera that was not developed for commercial purposes.

## 6. REFERENCES


Carvalho, L. A. S., Strauss C., and Fonseca, L. M. G. 2009. Determinação da resolução efetiva da camera HRC-CBERS-2B pelo método de espalhamento de borda. In: *XIV Simpósio Brasileiro de Sensoriamento Remoto*, Natal, Brazil, pp. 1975–1982.

Habib, A., Y. Lee, and M. Morgan, 2001. Bundle Adjustment with Self-Calibration of Line Cameras using Straight Lines. *Joint Workshop of ISPRS WG I/2, I/5 and IV/7: High Resolution Mapping from Space*, University of Hanover.

Habib, A., Morgan, M. and Lee, Y., 2002. Bundle Adjustment with Self-Calibration using Straight Lines. *Photogrammetric Record*, 17(100), pp. 635–650.

Habib, A. and Morgan, M. F., 2003. Linear Features in Photogrammetry. *Boletim de Ciências Geodésicas*, 9(1), pp. 3–24.

INPE. CBERS – China-Brazil Earth Resources Satellite. http://www.cbers.inpe.br/?hl=en&content=orbita1e2e2b (accessed 05 Apr. 2010).

Kim, T., and Dowman, I., 2006. Comparison of two physical sensor models for satellite images: Position-Rotation model and Orbit-Attitude model. *The Photogrammetric Record*, 21(114), pp. 110-123.

Kocaman, S. and A. Gruen, 2008. Geometric modeling and validation of ALOS/PRISM imagery and products. In: *The International Archives of Photogrammetry and Remote Sensing*, Vol. 37, Part B1, Beijing, pp. 731–737.

Light, D. L., Brown, D., Colvocoresses, A. P., Doyle, F. J., Davies, M., Ellasal, A., Junkins, J. L., Manent, J. R., Mckenney, A., Undrejka, R., and Wood, G, 1980. *Satellite Photogrammetry*, Manual of Photogrammetry (4th edition), Falls Church, USA: ASP, pp. 883-977.

Machado e Silva, A. J. F, 2007. Geometria de imagens: do projeto do satellite à geração dos produtos. Tese (Doutorado em Sensoriamento Remoto), Instituto Nacional de Pesquisas Espaciais, Sao Jose dos Campos, Brazil, 224 p.

Mikahil, E. M. and Ackerman, F., 1976. *Observations and Least Squares*. IEP, New York. 497 pages.

Mulawa, D. C. and Mikhail, E. M., 1988. Photogrammetric treatment of linear features. In: *The International Archives of Photogrammetry and Remote Sensing*, Vol. 27, Part B10, Kyoto, pp. III383–III393.

Orun, A. B. and Natarajan, K., 1994. A modified bundle adjustment software for SPOT imagery and photography: tradeoff. *Photogrammetric Engineering & Remote Sensing*, 60(12): 1431–1437.

Poli D. Modelling of Spaceborne Linear Array Sensors. Diss., Technische Wissenschaften ETH Zurich, Nr. 15894, 2005, IGP Mitteilung N. 85.

Tommaselli, A. M. G. and Tozzi, C. L., 1996. A recursive approach to space resection using straight lines. *Photogrammetric Engineering & Remote Sensing*, 62(1), pp. 57–66.

Tommaselli, A. M. G., and Medeiros, N. G. Determination of the indirect orientation of orbital images using control straight lines. To appear in Photogrammetric Record. July, 2010.

Toutin, T., and Rochon G. 1986. SPOT a new cartographic toll. In: *The International Archives of Photogrammetry and Remote Sensing*, Vol. 26, Part 4, Edinburgh, Scotland, pp. 192-205.

Toutin, T, 2003. Block Bundle Adjustment of Landsat 7 ETM+ Images over Mountainous Areas. *Photogrammetric Engineering & Remote Sensing*, 69(12), pp. 1341–1349.

Yu, J., Yuan X., and Zhenli W, 2008. Calibration of constant angular error for CBERS-2 imagery with few ground control points. In: *The International Archives of Photogrammetry and Remote Sensing*, Vol. 37, Part B1, Beijing, pp. 769–774.

## 7. ACKNOWLEDGEMENTS

The authors would like to acknowledge the support of FAPESP (Fundação de Amparo à Pesquisa do Estado de São Paulo) through a Master Scholarship (2009_03917-7), and CNPq (Conselho Nacional de Desenvolvimento Científico e Tecnológico) through Research Grants (307243/2007-9 and 477738_2009-5).